JOURNAL OF VIROLOGY, Dec. 1995, p. 7951–7959 Vol. 69, No. 12
0022-538X/95/$04.00+0

Envelopment of Varicella-Zoster Virus: Targeting of Viral Glycoproteins to the *trans*-Golgi Network

ZHENGLUN ZHU,[1] MICHAEL D. GERSHON,[1] YUE HAO,[1] RICHARD T. AMBRON,[1] CHRISTOPHER A. GABEL,[2] AND ANNE A. GERSHON[3]*

Departments of Anatomy and Cell Biology[1] and Pediatrics,[3] Columbia University College of Physicians and Surgeons, New York, New York 10032, and Department of Cancer Immunology and Infectious Disease, Pfizer Central Research, Groton, Connecticut 06340[2]

Received 20 June 1995/Accepted 12 September 1995

Previous studies suggested that varicella-zoster virus derives its final envelope from the *trans*-Golgi network (TGN) and that envelope glycoproteins (gps) are transported to the TGN independently of nucleocapsids. We tested the hypothesis that gpI is targeted to the TGN as a result of a signal sequence or patch encoded in its cytosolic domain. cDNAs encoding gpI wild type (wt) and a truncated mutant gpI(trc) lacking transmembrane and cytosolic domains were cloned by using the PCR. Cells transfected with cDNA encoding gpI(wt) or gpI(trc) synthesized and N glycosylated the proteins. gpI(wt) accumulated in the TGN, some reached the plasmalemma, but none was secreted. In contrast, gpI(trc) was retained and probably degraded in the endoplasmic reticulum; none was found on cell surfaces, but some was secreted. The distribution of gpI(trc) was not affected by deletion of potential glycosylation sites. To locate a potential gpI-targeting sequence, cells were transfected with cDNA encoding chimeric proteins in which the ectodomain of a plasmalemmal marker, the interleukin-2 receptor (tac), was fused to different domains of gpI. A chimeric protein in which tac was fused with the transmembrane and cytoplasmic domains of gpI was targeted to the TGN. In contrast, a chimeric protein in which tac was fused only with the gpI transmembrane domain passed through the TGN and concentrated in endosomes. We conclude that gpI is targeted to the TGN as a result of a targeting sequence or patch in its cytosolic domain.

Studies of the transport and modification of viral envelope proteins have made important contributions to the understanding of the pathways and mechanisms of viral maturation (11, 25). Insight into the steps by which a virus is assembled from its components can provide information that may ultimately lead to antiviral therapies. A critical element in the maturation of a virus is the mechanism by which the viral nucleocapsid becomes enclosed in an infection-competent membrane. The site of this envelopment may be determined by the targeting of the viral envelope glycoproteins (gps). For example, the E1 and E2 gps of rubella virus are transported to the Golgi region, which is believed to be the site of its envelopment (13, 14), whereas the gps of coronavirus, flavivirus, and rotavirus accumulate in the endoplasmic reticulum (ER), which is thought to provide the envelope for these virions (23). The most extensively investigated of the alphaherpesviruses has been herpes simplex virus; however, the site at which herpes simplex viruses are enveloped is controversial. Electron microscopic observations first suggested the hypothesis that the viruses acquire an envelope while budding through the inner nuclear membrane (5, 20, 21). This idea has received considerable support; thus, herpes simplex virus gps have been localized to the nuclear membrane by immunofluorescence, immunoelectron microscopy, and subcellular fractionation (3, 5, 25). Unfortunately, however, studies of the localization of herpes simplex virus gps have not been able definitively to exclude the possibility that the gps are located in the outer, rather than the inner, nuclear membrane. Since the outer nuclear membrane is continuous with the ER, the localization of gps in the nuclear envelope could reflect only their site of biosynthesis and not targeting related to viral envelopment. A second alphaherpesvirus, pseudorabies virus, has been reported to be assembled in two stages (27): a primary envelope is acquired as the nucleocapsids bud through the inner nuclear membrane; however, this envelope is lost as the nucleocapsids penetrate the ER to enter the cytosol, and the secondary (final) envelope is acquired within the Golgi apparatus.

A prior study of the maturation of varicella-zoster virus (VZV) has indicated that the process is similar to that proposed for pseudorabies virus (9). After the VZV nucleocapsid is assembled in the nucleus, it acquires a temporary envelope by budding through the inner nuclear membrane. This budding delivers the newly enveloped virions to the perinuclear space, which is continuous with the lumen of the ER. Virions in the ER fuse with the ER membrane, releasing nucleocapsids into the cytosol. The nucleocapsids migrate to the *trans*-Golgi network (TGN), where they acquire a second and final envelope. An important feature of this model is that the envelope gps of VZV are processed separately from the nucleocapsids. These gps follow the ER→Golgi route along which they are glycosylated and acquire mannose 6-phosphate (Man 6-P) residues (7). The mature gps are then united with the nucleocapsids in the TGN (9). This pathway suggests that the gps of VZV may be targeted to the TGN in which they accumulate prior to viral envelopment. The current study was undertaken to test the hypothesis that gps of VZV are targeted to the TGN as a result of an intrinsic signal sequence present in the cytosolic domain of these molecules.

MATERIALS AND METHODS

PCR cloning. The VZV gpI gene was cloned from VZV genomic DNA of the Ellen strain. Amplification of the full-length gpI gene was performed with the primers 5′-CCCGGTACCGAGGGTCGCCTGTAATAT-3′ (VZGP1L5) and 5′-CCCTCTAGATGCCCCGGTTCGGTGATCA-3′ (VZGP1L3), which flank the open reading frame of the gpI gene (6). A truncated form of the gpI gene, which lacks the cytoplasmic and membrane-spanning domains, was amplified with primers VZGP1L5 and 5′-CCCTCTAGATAGTCGCCGGTGGCTGA CC-3′ (VZGP1S3). Amplifications were performed as described previously (17).

* Corresponding author.

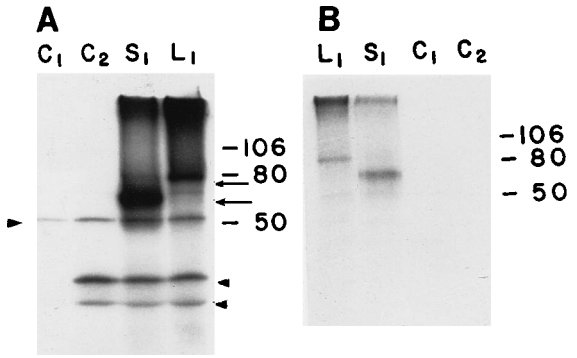

FIG. 1. (A) In vitro translation. Polypeptides were generated from cDNAs encoding gpI(wt) and gpI(trc) by in vitro translation in media containing [^{5}S]methionine. The products of in vitro translation were analyzed by SDS-PAGE. Lanes: C1, control, reaction mixture only, no plasmid was added; C2, control, only the plasmid vector was added; S1, plasmid containing cDNA encoding gpI(trc) was added; L1, plasmid containing cDNA encoding gpI(wt) was added. The arrows indicate the positions of specific translation products corresponding to the 60-kDa gpI(trc) and the 80-kDa gpI(wt). The specific translation products are not seen in the control lanes. Nonspecific translation products of lower molecular size are also present in the control lanes (arrowheads). (B) Immunoprecipitation of in vitro translation products. The authenticity of the identification of the products of in vitro translation was verified by immunoprecipitation with a human antiserum to VZV (7, 9). Lanes: L1, reaction mixture to which the plasmid containing cDNA encoding gpI(wt) was added; S1, reaction mixture to which the plasmid containing cDNA encoding gpI(trc) was added; C1, control reaction mixture to which no plasmid vector was added; C2, control reaction mixture to which no plasmid was added. Specific immunoprecipitates of the appropriate sizes were found only in lanes L1 and S1.

After an initial incubation for 3 min at 94°C, reaction mixtures were subjected to 35 of the following cycles: 1 min at 94°C, 1 min at 58°C, and 3 min at 72°C.

Two-thirds of the PCR-amplified DNA in TE buffer (10 mM Tris [pH 7.4], 1 mM EDTA) was digested with *Asp*718 and *Xba*I. After gel purification, the digested PCR fragments were cloned into the multiple cloning sites of the eucaryotic expression vector, pSVK3 (Pharmacia, Piscataway, N.J.), which had been digested with the same enzymes. After ligation, *Escherichia coli* (DH5α) was transformed with the plasmids. Positive clones were selected by small-scale DNA preparation and restriction enzyme digestion with *Asp*718 and *Xba*I. Plasmid DNA from selected subclones was amplified and purified by CsCl gradient centrifugation. The authenticity of all constructs was verified by sequencing, using a kit (Sequenase version 2.0; U.S. Biochemical Corp., Cleveland, Ohio). Authenticity of cloned cDNA encoding gpI wild type (wt) and a truncated mutant gpI(trc) was also verified by in vitro translation (Fig. 1A), which was carried out using a transcription and translation coupling kit (rabbit reticulocyte lysate system; Promega Biotec) according to the manufacturer's instructions. Translated proteins were identified by immunoprecipitation. In vitro translation products were diluted 1:10 with buffer (100 mM NaCl, 1% Triton X-100, 0.5% deoxycholate, 5 mM β-glycerophosphate) and immunoprecipitated with human anti-VZV polyclonal antibody (1:100). After 2 h on ice, protein G-Sepharose (Calbiochem, San Diego, Calif.) was added, and 30 min later the resulting precipitate was pelleted by centrifugation. After washing with buffer (10 mM Tris [pH 7.0], 1 mM EDTA, 0.1% sodium dodecyl sulfate [SDS], 1% Triton X-100, 0.4% deoxycholate), the immune complex was released from protein G by adding Laemmli sample buffer (LSB) and boiling for 5 min. Immunoprecipitates were analyzed by SDS-polyacrylamide gel electrophoresis (PAGE) and visualized by fluorography (Fig. 1B).

Deletion of glycosylation sites and preparation of chimeric proteins. cDNA constructs were prepared, encoding gpI mutants in which glycosylation sites were deleted as well as chimeric proteins in which domains of gpI were fused to the extracellular domain of the human interleukin-2 receptor (tac). Schematic representations of the constructs prepared are shown in Fig. 2. Methods used were essentially those described by Ho et al. (12) and Sharon et al. (24). In the first step, two overlapping DNA fragments were amplified by the terminal primers and overlapping internal primers encompassing the designed mutant. The products of this first round of amplification were gel purified and used for a second round of PCR amplification in which only the terminal primers were used. The terminal primers were VZGP1L5 and VZGP1S3 (defined above). The internal primers were as follows: glycosylation site 1, 5′-ATTGTTGTAAACACGG GCACACTGTTTGA-3′ and 5′-CAGTGTGCCCGTGTTTA-3′; glycosylation site 2, 5′-AAAACAAGAAACCCTGCGCCCGCAGTAACT-3′ and 5′-TGC GGGCGCAGGCTTTC-3′; and glycosylation site 3, 5′-CATGCAGATAACT ACGCCGCATATTGTCTG-3′ and 5′-ATATGCGGCGTAGTTAT-3′. For preparation of fusion proteins, the terminal 5′ tac primer was 5′-CCCGGTACC AAGGGTCAGGAAGATGGA-3′, which was paired with VZGP1L3. The internal primers were 5′-GGGGGTAATTTCTGTTGTAAATATGGACGT-3′ and 5′-TTTACAACAGAAATTACCCCCGTAAAC-3′.

Transfection of cells. Cos-7 cells were grown in Dulbecco's modified Eagle's medium (DMEM) containing heat-inactivated 10% fetal bovine serum (FBS), 100 U of penicillin per ml, and 100 U of streptomycin per ml. Cultures were maintained at 37°C with 5% CO_2. Transfection was performed by electroporation. Cos-7 cells (10^7) were released from dishes with trypsin (0.5 ml). Trypsinization was stopped by adding 0.5 ml of cold electroporation buffer (DMEM, 10% bovine calf serum, 20 mM HEPES [*N*-2-hydroxyethylpiperazine-N′-2-ethanesulfonic acid]). A cell suspension (0.8 ml, containing 10^7 cells per ml) was transferred into a 0.4-cm gap cuvette (Bio-Rad Laboratories, Richmond, Calif.), and 40 μg of DNA was added. After incubation on ice for 5 min, the cuvette was placed in the chamber of a Gene Pulser electroporation unit (Bio-Rad Laboratories) and pulsed at 300 V, 960 μF. After electroporation, the cuvette was put on ice for 5 min and then the cells were transferred to a 10-cm tissue culture dish containing growth medium. After 12 h, the media were changed and incubation was continued for another 48 h at 37°C with 5% CO_2.

Immunocytochemistry. Transfected cells growing on cover slides in a six-well tissue culture dish were fixed with 2% formaldehyde (freshly prepared from paraformaldehyde) for 2 h at room temperature. The cells were washed with phosphate-buffered saline (PBS) and some were permeabilized with 0.1% Triton X-100 in PBS. The cells were then exposed either to mouse anti-VZV gpI (kindly supplied by Charles Grose) or to mouse anti-tac monoclonal antibodies (1:100 diluted with PBS–2 mg of bovine serum albumin [BSA] per ml; Amersham Corp., Arlington Heights, Ill.) for 2 h at room temperature. After rinsing with PBS, the cultures were exposed to fluorescein isothiocyanate- or tetramethyl rhodamine isothiocyanate (TRITC)-labeled goat anti-mouse immunoglobulin G (1:80 diluted with PBS–2 mg of BSA per ml) (Kirkegaard & Perry, Gaithersburg, Md.), washed in PBS, and mounted in the presence of β-nitrophenol, to minimize fading. Antibodies to the large cation-independent Man 6-P receptor (MPR^{ci}) (7, 9, 16) enabled the TGN to be identified (1). Although the MPR^{ci} is also located in prelysosomes (late endosomes) (4, 10), which are visible when MPR^{ci}

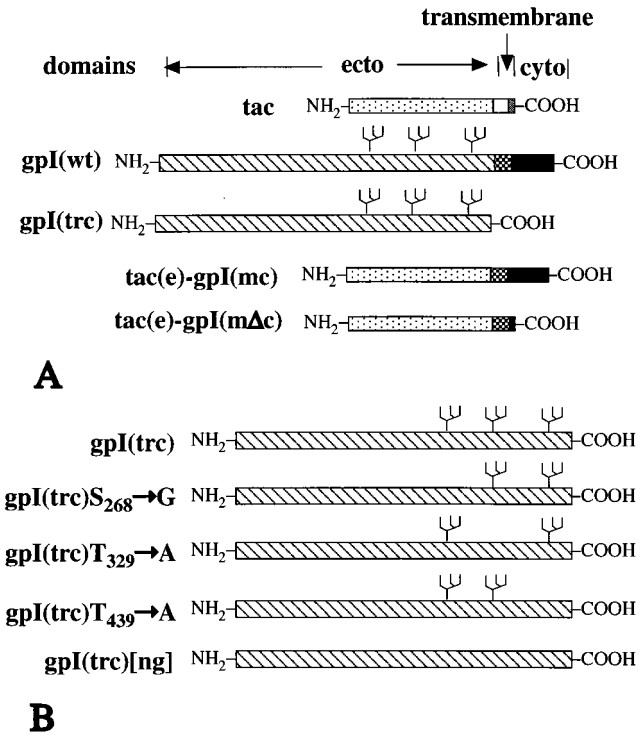

FIG. 2. Constructs used to transfect cells in this study. (A) Schematic presentation of the full-length tac, gpI(wt), gpI(trc), and chimeric proteins tac(e)-gpI(mc), in which the extracellular domain of tac was fused to the transmembrane and cytosolic domains of gpI, and tac(e)-gpI(mΔc), in which the extracellular domain of tac was fused only to the transmembrane domains of gpI. The approximate positions of potential glycosylation sites on the extracellular domain of gpI are indicated. The open region in tac, and the checkered regions in gpI(wt), and the chimeric proteins show the position of the presumed transmembrane domains of the molecules. (B) Schematic presentation of gpI(trc) mutants in which potential glycosylation sites were deleted individually or all together, gpI(trc)[ng].

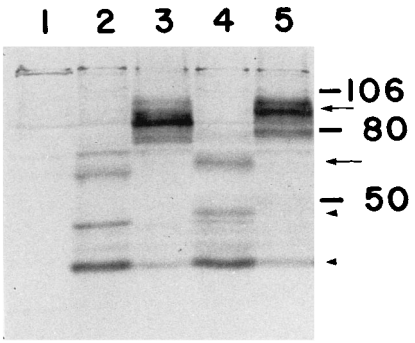

FIG. 3. Immunoblots indicate that transfected cells synthesize and glycosylate gpI(wt) or gpI(trc). Cos-7 cells were transfected with cDNA encoding either gpI(trc) (lanes 2 and 4) or gpI(wt) (lanes 3 and 5). The cells were either incubated in unsupplemented growth medium for 60 h (lanes 4 and 5) or incubated in unsupplemented growth medium for 48 h and then changed to medium containing 10 mM tunicamycin for an additional 12 h (lanes 2 and 3). After incubation, cellular proteins were extracted, resolved by SDS-PAGE, blotted onto nitrocellulose, and probed with antibodies to gpI. The arrows show the position of gpI(trc) (lane 4) and gpI(wt) (lane 5) from non-tunicamycin-treated cells. Note that tunicamycin causes both gpI(trc) (lane 2) and gpI(wt) (lane 3) to shift to a lower apparent molecular weight. Note that small-sized gpI-immunoreactive products of evident degradation are also present (arrowheads), especially for gpI(trc) (lanes 2 and 4). No gpI-immunoreactive proteins were detected in cells that were not transfected (lane 1).

immunoreactivity is demonstrated, its concentration in the TGN permits that organelle to be visualized. A second TGN marker was the lipid *N*-(ε-7-nitrobenz-2-oxa-1,3-diazo-4-*yl*-aminocaproyl)-D-*erythro*-sphingosine (C_6-NBD-Cer), which concentrates in the TGN (22). Double labeling was carried out with primary antibodies raised in different species in combination with appropriate species-specific secondary antibodies. Immunoreactivity was visualized by vertical fluorescence microscopy. TRITC fluorescence was viewed with a dichroic mirror-filter cube (exciting filter BP 530-560; dichroic mirror RKP 580; barrier filter LP 580) that passed no fluorescein isothiocyanate fluorescence. Fluorescein isothiocyanate fluorescence was viewed with a narrow band dichroic mirror-filter combination (exciting filter BP 450-490; dichroic mirror RKP 510, barrier filter BP 525/20) that passed no TRITC fluorescence.

Immunoblotting. Transfected and control cells were collected and rinsed with PBS, and the cell pellets were boiled in LSB for 5 min. For analysis of release of protein into tissue culture fluid (TCF), the final 12 h of incubation were carried out in a serum-free medium consisting of modified Eagle's medium with 0.5% FBS. The TCF was collected, clarified by centrifugation, lyophilized, and extracted into LSB as described above. Proteins in the LSB were separated by SDS-PAGE and then electroblotted onto nitrocellulose paper by using a transfer buffer (150 mM NaCl, 10 mM 3-[cyclohexylamino]-1-propanesulfonic acid [CAPS], 10% methanol). Nonspecific binding was blocked with PBS containing 5% non-fat dry milk. Blots were then incubated with mouse anti-VZV gpI monoclonal antibodies (1:2000; diluted with PBS–3% dry milk) for 2 h, and immunoreactivity was demonstrated with peroxidase-conjugated rabbit anti-mouse antibody (diluted 1:1000) and visualized by incubation with 3-3′-diaminobenzidine.

RESULTS

gpI(wt) and gpI(trc) are glycosylated in transfected Cos-7 cells. In initial experiments, Cos-7 cells were transfected either with a construct that encoded the full-length gpI(wt) or with a construct that encoded the truncated product gpI(trc), from which both the membrane-spanning and cytosolic domains were deleted (Fig. 2A). Immunoblots were prepared at 60 h after transfection. Essentially, no gpI-immunoreactive protein was found in control cells, which were not transfected with either construct (Fig. 3, lane 1). The major gpI-immunoreactive polypeptides found in cells transfected with gpI(wt) ranged in size from 80 to 95 kDa (Fig. 3, lane 5). This size variation is likely to reflect variable amounts of glycosylation of the expressed protein, because no immunoreactive protein in this size range was observed when transfected cells were exposed to tunicamycin (10 μM; Fig. 3, lane 4); tunicamycin treatment caused a band shift of about 10 kDa. The major gpI-immunoreactive polypeptides found in cells transfected with the gpI(trc) ranged in size from 60 to 70 kDa (Fig. 3, lane 3). As occurred with cells transfected with cDNA encoding the full-length gpI(wt), tunicamycin treatment of cells transfected with the gpI(trc) caused a band shift of about 10 kDa (Fig. 3, lane 2). Lower molecular size breakdown products were also observed in immunoblots, especially when cells were treated with tunicamycin. These data indicate that both the full-length, gpI(wt), and the gpI(trc) are synthesized and glycosylated in Cos-7 cells transfected with the corresponding cDNAs. Both products, therefore, are probably translated on attached polyribosomes and cotranslationally translocated through the membrane of the ER to permit the polypeptide chains to be glycosylated within the lumen. These results are consistent with hydropathy plots (not illustrated), which suggest that gpI contains an N-terminal signal sequence. Subsequent processing of the gpI(wt) and gpI(trc) proteins, however, appeared to differ.

gpI(trc) is degraded to a greater extent than gpI(wt) and is secreted. More breakdown products were observed when cells were transfected with the gpI(trc) than with the gpI(wt) (Fig. 4); moreover, gpI(trc) disappeared at a more rapid rate than gpI(wt) when transfected cells were incubated in the presence of cyclohexamide (not illustrated). gpI(trc), therefore, was less stable in transfected cells than was gpI(wt). To determine whether gpI(wt) or gpI(trc) was secreted, TCF was collected from the transfected cells and analyzed by SDS-PAGE. A 75-kDa band was detected in the TCF of cells transfected with the gpI(trc) (Fig. 4, lane 5). Since the size of this polypeptide was larger than that of the cell-associated gpI(trc), this protein must have traversed the Golgi complex and acquired sugar residues en route to secretion. Similarly, since the size of cell-associated gpI(trc) was smaller than that which was secreted, the bulk of this material must not have traversed the Golgi apparatus. In contrast, no band was detected in the TCF ob-

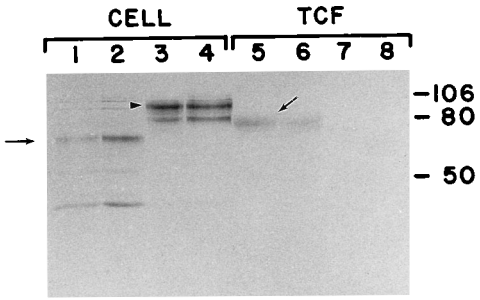

FIG. 4. gpI(trc), but not gpI(wt), is secreted. Cos-7 cells were transfected with cDNA encoding either gpI(trc) (lanes 1, 2, 5, and 6) or gpI(wt) (lanes 3, 4, 7, and 8). Cells were incubated for 48 h after transfection and then for an additional 12 h in a medium in which the FBS concentration was reduced to 0.5%. After incubation, cellular proteins were extracted, resolved by SDS-PAGE, blotted onto nitrocellulose, and probed with antibodies to gpI (lanes 1 to 4). In addition the medium (TCF) was also collected and similarly analyzed (lanes 5 to 8). Experimental cells were treated with chloroquine (100 μM), which was present during the final 12 h of incubation (lanes 2, 4, 6, and 8). Note that chloroquine induced an apparent increase in the density of the gpI-immunoreactive protein obtained from cells transfected with cDNA encoding gpI(trc) (compare lane 2 [chloroquine] with lane 1). No change followed treatment with chloroquine when cells were transfected with gpI(wt) (compare lane 4 [chloroquine] with lane 3). Secretion of gpI(trc) has occurred, since this gpI(trc) (↙) is present in the medium of cells transfected with cDNA encoding gpI(trc) (lanes 5 and 6). The evident secretion of gpI(trc) is reduced by chloroquine (compare lane 6 [chloroquine] with lane 5). No secretion of gpI(wt) can be detected either in the absence (lane 7) or presence of chloroquine (lane 8). The arrow on the left indicates the position of the full-length gpI(trc) and the arrowhead indicates the position of the full-length gpI(wt).

tained from cells transfected with gpI(wt) (Fig. 4, lane 7). gpI(trc), but not gpI(wt), therefore, is secreted.

Since the carbohydrate chains of gpI contain Man 6-P (7), it is conceivable that the gpI(trc) could, like lysosomal enzymes, which also acquire Man 6-P, bind to an MPR (15, 16). Binding of the gpI(trc) to an MPR, if it occurred, would be expected to target the gpI(trc) to lysosomes, a process that could account for the greater breakdown of the gpI(trc) than of the gpI(wt). The gpI(wt) is an integral membrane protein and thus might not be sorted by binding to an MPR in the same way as lysosomal enzymes, which are free proteins in the cisternal space. To determine whether an intracellular MPR might be involved in targeting of the gpI(trc), we incubated transfected cells with chloroquine (100 μM) in order to alkalinize internal compartments, interfere with the trafficking of MPRs, and prevent diversion of gpI(trc) from the secretory pathway to the endosomal pathway (7, 16). Treatment of transfected cells with chloroquine for 12 h did not promote secretion of the gpI(trc); instead, secretion was inhibited (Fig. 4, lane 6). The decrease in gpI(trc) secretion was accompanied by a chloroquine-induced increase in the amount of gpI(trc) that remained cell associated (Fig. 4, lane 2). Since alkalinization by chloroquine inhibits degradation of proteins in lysosomes, the increase in intracellular gpI(trc) could have resulted from protection of gpI(trc) in lysosomes. Alternatively, chloroquine might have reduced secretion of the gpI(trc) nonspecifically, by retarding its intracellular transport. In order to distinguish between these possibilities, we deleted all three potential glycosylation sites from gpI(trc) (Fig. 2B, gpI(trc)[ng]). Cos-7 cells were then transfected with cDNA encoding the glycosylation site-deleted variant, gpI(trc)[ng], and we determined the effect of chloroquine on its breakdown and secretion. Like gpI(trc), gpI(trc)[ng] was secreted; however, in contrast to gpI(trc), the size of the secreted gpI(trc)[ng] was not larger than that of the cell-associated protein, confirming that sugar residues were not added to gpI(trc)[ng] in the Golgi apparatus prior to secretion (data not illustrated). Again, chloroquine inhibited the secretion of gpI(trc)[ng] and increased the proportion that was cell associated. These observations suggest that the effects of chloroquine are antisecretory and do not support the idea that the gpI(trc) is diverted by an MPR from the secretory pathway to lysosomes.

Localization of the gpI(wt) and the gpI(trc) in transfected Cos-7 cells. We tested the hypothesis that intracellular targeting of gpI(wt) is dependent on a sequence or patch located in the putative cytosolic domain of gpI (Fig. 2A). Since gpI(trc) retains the N-terminal ER-directing signal sequence of the gpI(wt) but lacks the likely hydrophobic membrane-spanning and cytosolic domains, it would be expected to be a soluble intracisternal protein and targeted differently from gpI(wt), which is an integral membrane protein. In order to test the role of the probable membrane-spanning and cytosolic domains of gpI(wt), Cos-7 cells were transfected with cDNA encoding either gpI(wt) or gpI(trc) and the respective proteins were located immunocytochemically by using an antibody to gpI. The immunoreactivity of the MPR^{ci} was studied simultaneously in the same cells and served as a TGN marker. The location of C_6-NBD-Cer was also determined and utilized as a second TGN marker. In permeabilized cells transfected with cDNA encoding gpI(wt), intracellular gpI immunoreactivity was highly concentrated in a Golgi pattern that coincided with the location of MPR^{ci} immunoreactivity (Fig. 5A and B). This pattern suggests that gpI(wt) is targeted to the TGN. In contrast, in cells transfected with cDNA encoding gpI(trc), most gpI immunoreactivity was located in the ER (Fig. 5C) and only small amounts codistributed with MPR^{ci} immunoreactivity (Fig. 5D). The location of gpI immunoreactivity was also coincident with that of C_6-NBD-Cer in cells transfected with cDNA encoding gpI(wt) (Fig. 5E and F) but not in cells transfected with cDNA encoding gpI(trc) (Fig. 5G and H). When antibodies to gpI were applied to cells that had not been permeabilized, cell surface gpI immunoreactivity was found on cells that had been transfected with cDNA encoding gpI(wt) (Fig. 6A) but not on those transfected with cDNA encoding gpI(trc) (Fig. 6B). These observations are consistent with, but not proof of, the hypothesis that there is a targeting signal in the cytosolic domain of gpI(wt). Although the protein synthesized in cells transfected with gpI(trc) did not, like that in cells transfected with cDNA encoding gpI(wt), accumulate in the TGN, a role in targeting of a sequence in the transmembrane domain of gpI is not excluded by these data.

The possibility that N glycosylation might affect the intracellular targeting of the intracisternal protein gpI(trc) was investigated by mutating each of the potential glycosylation sites of this protein individually or all three together (Fig. 2B). The apparent molecular sizes, ~55 kDa, of gpI(trc)S_{268}→G and that of gpI(trc)T_{439}→A were each found to be about 5 to 8 kDa lower than that of gpI(trc), ~65 kDa. In contrast, the apparent molecular size, ~65 kDa, of gpI(trc)T_{329}→A was identical to that of gpI(trc); moreover, the apparent molecular size of gpI(trc)[ng], which lacks all three potential glycosylation sites was about 10 to 16 kDa lower than that of either gpI(trc) or gpI(trc)T_{329}→A. These observations suggest that only two of the three potential glycosylation sites of gpI(trc) are actually used. The distribution of gpI immunoreactivity in cells that were transfected with each of the glycosylation site-deficient mutants could not be distinguished from that observed in cells transfected with gpI(trc) itself (data not illustrated). These observations do not support the hypothesis that N glycosylation affects the trafficking of gpI(trc).

The TGN targeting signal of gpI(wt) is located in its cytosolic domain. To distinguish a possible role in targeting of cytosolic and transmembrane domains of gpI, we prepared cDNA constructs encoding chimeric proteins in which the extracellular domain of the plasma membrane marker protein, tac was fused either to the entire region, encompassing both the transmembrane and cytosolic domains of gpI [Fig. 2A, tac(e)-gpI(mc)], or only to the transmembrane domain of gpI [Fig. 2A, tac(e)-gpI(mΔc)]. Cos-7 cells were then transfected with these constructs or with cDNA encoding the full-length sequence of tac, and the distribution of the corresponding proteins was investigated immunocytochemically with antibodies that reacted with the extracellular domain of tac. tac-immunoreactivity protein accumulated on the surfaces of cells transfected with the full-length cDNA encoding tac, and very little immunoreactivity was observed intracellularly (Fig. 7A). In contrast, tac immunoreactivity accumulated in the Golgi region of cells transfected with cDNA encoding the chimeric protein, tac(e)-gpI(mc), in which both the transmembrane and cytosolic domains of gpI were fused to the extracellular domain of tac (Fig. 7B). Small immunoreactive vesicles were also present but were rare, although some tac-immunoreactive protein was also detected at the cell surface. When cells were transfected with cDNA encoding the chimeric protein, tac(e)-gpI(mΔc), in which only the transmembrane domain of gpI was fused to the extracellular domain of tac, immunoreactivity did not accumulate in the Golgi region but instead was distributed in small vesicles that were scattered throughout the cytoplasm (Fig. 7D). Double-label immunocytochemistry was used to identify the structures in which tac immunoreactivity accumulated in cells transfected with cDNA encoding the chimeric proteins. The tac immunoreactivity in cells transfected with

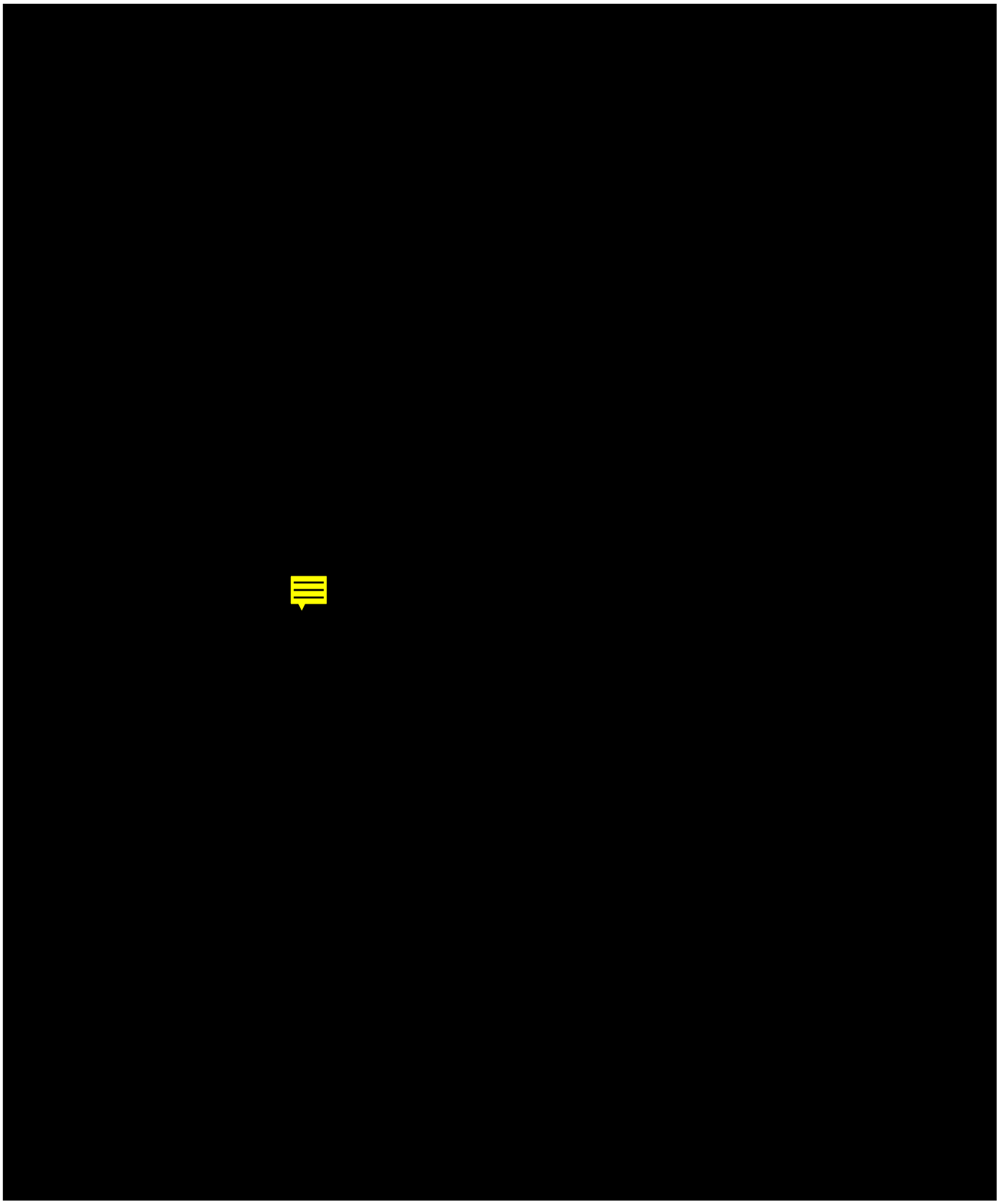

FIG. 5. The intracellular distribution of gpI immunoreactivity coincides with MPR^{ci} immunoreactivity and C_6-NBD-Cer in cells transfected with cDNA encoding gpI(wt) but not gpI(trc). Cos-7 cells were transfected with cDNA encoding gpI(wt) (A and B, E and F) or gpI(trc) (C and D, G and H). The immunoreactivity of the MPR^{ci} (B and D) and the distribution of C_6-NBD-Cer (F and H) served as TGN markers and were visualized simultaneously with gpI immunoreactivity (A, C, E, and G). In cells transfected with cDNA encoding gpI(wt), gpI immunoreactivity was colocalized with MPR^{ci} immunoreactivity (compare panel A, gpI, with panel B, MPR^{ci}) and with C_6-NBD-Cer (compare panel E, gpI, with panel F, C_6-NBD-Cer). No colocalization of the two TGN markers with gpI immunoreactivity was evident in cells transfected with gpI(trc) (compare panel C, gpI, with panel D, MPR^{ci}, and panel G, gpI, with panel H, C_6-NBD-Cer). Corresponding TGN regions in each pair of micrographs are marked by arrows. The pattern of gpI immunoreactivity in cells transfected with cDNA encoding gpI(trc) (C and G) resembles that of the ER, suggesting that there may be relatively little transport of gpI(trc) out of this organelle. Bars, 20 μm.

cDNA encoding tac(e)-gpI(mc) (the transmembrane and cytosolic domains of gpI fused to the extracellular domain of tac) displayed a coincident localization both with C_6-NBD-Cer (Fig. 7E and F) and with MPR^{ci} immunoreactivity (not illustrated). In order to determine whether the small vesicles containing tac immunoreactivity in cells transfected with cDNA encoding tac(e)-gpI(mΔc) (only the transmembrane domains of gpI fused to the extracellular domain of tac) were endosomes, Cos-7 cells were incubated for 1 h with α-macroglobulin coupled either to fluorescein isothiocyanate or to the red fluorescent dye, Cy3, prior to transfection in order to prelabel structures accessible to an endosomal marker. The small tac-immunoreactive vesicles were found to contain fluorescent α-macroglobulin (Fig. 7G and H). These data suggest that the TGN-targeting domain of gpI resides in its cytosolic domain.

DISCUSSION

The current experiments were undertaken to test the hypothesis that gpI is targeted to the TGN because of a signal contained in the sequence of the molecule. To do so, Cos-7 cells were transfected with a variety of cDNA constructs so that the intracellular sorting and targeting of gpI could be investigated independently of other virally encoded products. gpI was selected for study because it is the most abundant gp of the VZV envelope (19). Although gpI is thus a good model, there was no reason to suspect that gpI plays a greater role in viral envelopment than any of the other gps of the viral envelope. The data indicated that cells transfected with cDNA encoding the full-length gpI(wt) synthesize and glycosylate the protein but do not secrete it. Immunocytochemical observations demonstrated that the gpI(wt) synthesized in the transfected cells accumulated in the Golgi region and reached the plasma membrane. Since the gpI-immunoreactive protein in the Golgi region coincided in its location with those of MPR^{ci} immunoreactivity and C_6-NBD-Cer, it was concluded that gpI(wt) is targeted to the TGN. Since no other products encoded by the VZV genome are expressed in transfected cells, the observations provide support for the hypothesis that the information required for the targeting of gpI(wt) is present in the sequence of this protein.

In order to determine which domain of the gpI(wt) sequence is responsible for its trafficking to the TGN, cells were transfected with cDNA encoding a mutant, gpI(trc), that lacked the putative transmembrane and cytosolic domains. Cells synthesized and glycosylated this protein, demonstrating that it is produced on ribosomes attached to the ER and translocated to the cisternal space. In contrast to gpI(wt), however, gpI(trc) was secreted, suggesting that, as expected, the protein was not an integral membrane protein but free in the cisternal space. Since the secreted form of the gpI(trc) was somewhat larger than the cell-associated protein, it is likely that additional sugar residues were added to gpI(trc) in the Golgi apparatus prior to secretion (16). Since gpI(trc) was less stable in transfected cells than was gpI(wt), we investigated the possibility that gpI(trc) is partially diverted to the lysosomal pathway. The potential for such a diversion arises because VZV gps have been demonstrated to acquire Man 6-P and thus might bind to an MPR (7); moreover, gps of HSV have also been recently observed to acquire Man 6-P in transfected cells and to bind to MPRs (2). Despite the glycosylation of gpI(trc), however, no evidence could be obtained to indicate that glycosylation plays an important role in the trafficking of this molecule. The weak base, chloroquine, did decrease the proportion of secreted gpI(trc) and increase that which remained cell associated; nevertheless, chloroquine exerted the same effect on the distribution of secreted and cell-associated protein synthesized by cells transfected with cDNA encoding a variant of gpI(trc) in which all three potential glycosylation sites were deleted. In addition, the intracellular distribution of gpI-immunoreactive protein in cells transfected with variants of gpI(trc), in which each of the potential glycosylation sites was mutated, individually, or all together, was indistinguishable from that of gpI(trc) itself. The intracellular distribution of gpI(trc) was quite different from that of gpI(wt). In contrast to gpI(wt), gpI(trc) did not accumulate in the Golgi (TGN) region and did not reach the plasma membrane. The failure of gpI(trc) to reach the cell surface is consistent with the idea that it becomes free in the cisternal space and does not associate with membranes. The failure of gpI(trc) to accumulate in the region of the TGN implies that the domain(s) of the molecule responsible for targeting the protein to this structure have been deleted. The bulk of gpI(trc) within cells appeared, on the basis of immunocytochemical observations, to be retained in the ER. It seems likely that this abnormal molecule is recognized as such in transfected cells and is largely retained and degraded in the ER (18), accounting for the greater instability of this gpI(trc) than gpI(wt). Subsequent studies were thus carried out with constructs encoding chimeric integral membrane proteins that would more closely resemble gpI(wt) than gpI(trc).

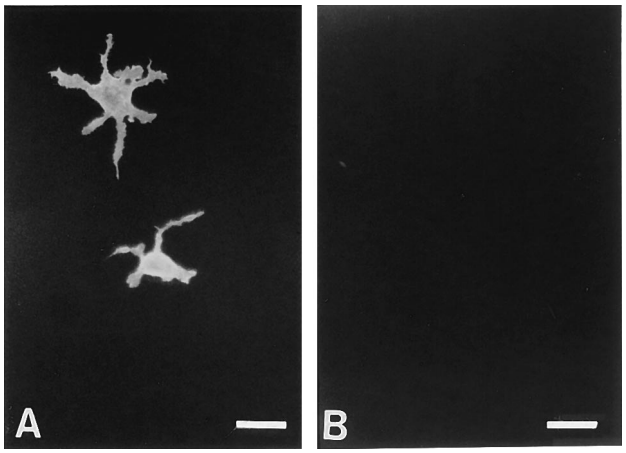

FIG. 6. gpI immunoreactivity reaches the surfaces of cells transfected with cDNA encoding gpI(wt) but not gpI(trc). Cells were transfected with either gpI(wt) (A) or gpI(trc) (B) and examined immunocytochemically without permeabilization. As a result, only cell surface immunoreactivity is detectable. Note that the surfaces of cells transfected with gpI(wt) display gpI immunoreactivity (A), but no gpI immunoreactivity appears on the surfaces of similarly treated cells transfected with gpI(trc) (B). Bars, 20 μm.

Constructs encoding chimeric molecules were employed to distinguish the role in the targeting of gpI of its transmembrane and cytosolic domains. The extracellular domain of tac was fused to either the transmembrane domain of gpI or to both its transmembrane and cytosolic domains. As expected tac-immunoreactive protein was targeted to the plasma membrane in control cells transfected with cDNA encoding the full-length tac. In cells transfected with cDNA encoding the chimeric tac(e)-gpI(mc), in which the extracellular domain of tac was fused to the transmembrane and cytosolic domains of gpI, however, the distribution of tac-immunoreactive protein was the same as that of gpI-immunoreactive protein in cells transfected with gpI(wt). As a result, tac-immunoreactive protein displayed a coincident distribution with those of the TGN markers, MPR^{ci} immunoreactivity, and C_6-NBD-Cer. In contrast, in cells transfected with tac(e)-gpI(mΔc), in which the

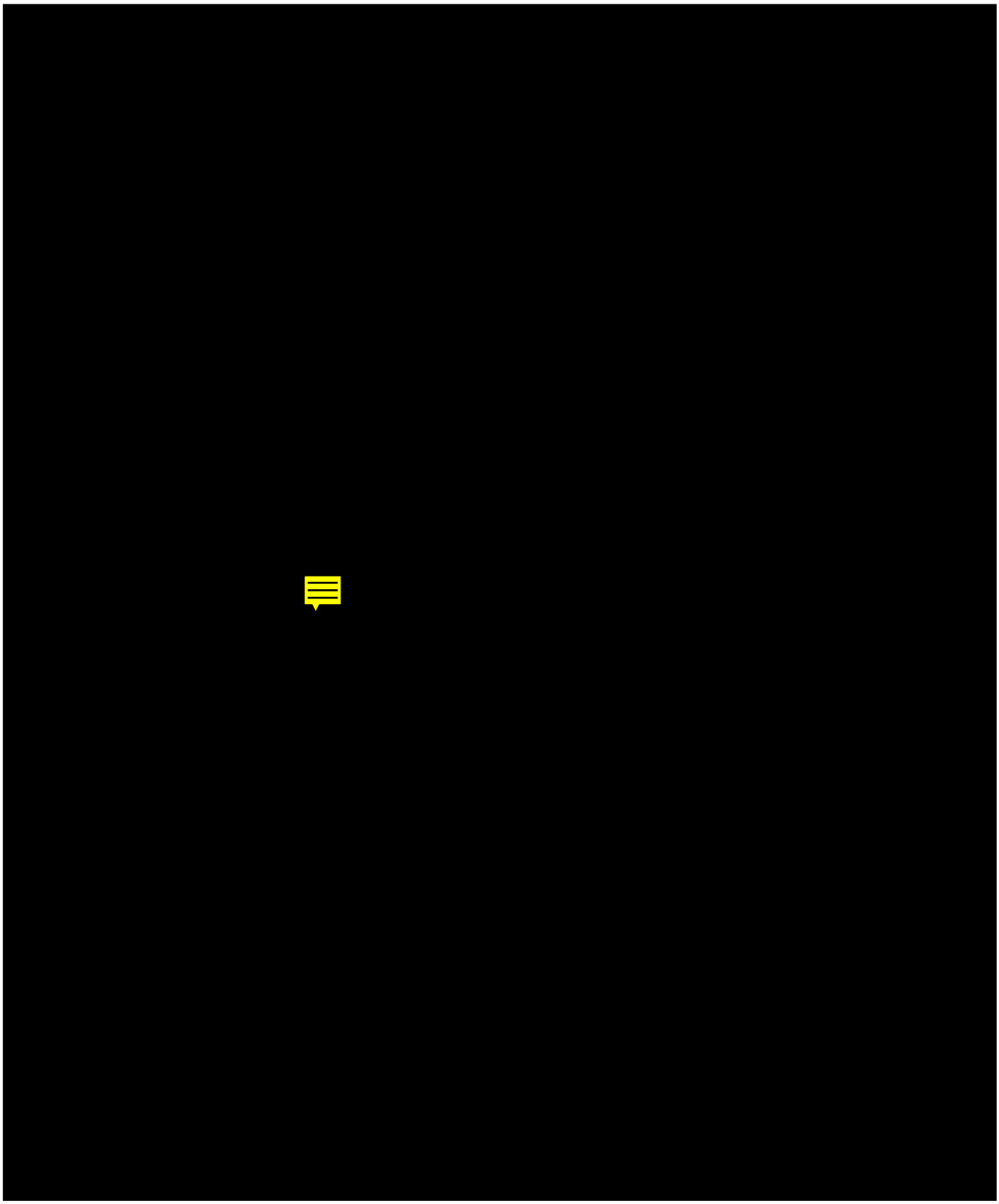

FIG. 7. The cytosolic domain of gpI contains all the information needed to target the protein to the TGN. Cells were transfected with cDNA encoding tac or with constructs encoding chimeric proteins in which the extracellular domain of tac [tac(e)] was fused to the transmembrane and cytosolic (mc) domains of gpI or only to the gpI transmembrane domain (mΔc). (A) In cells transfected only with cDNA encoding tac, the tac immunoreactivity concentrates on the cell surface. (B and C) In cells transfected with the construct tac(e)-gpI(mc), tac immunoreactivity (arrows) is concentrated in the Golgi region. Small numbers of cytoplasmic tac-immunoreactive vesicles are also found. (D) In cells transfected with the construct, tac(e)-gpI(mΔc), tac immunoreactivity is concentrated in small cytoplasmic vesicles and does not accumulate in the Golgi region (compare with panel C). (E and F) The region of cells in which tac immunoreactivity accumulates (E, arrows) in cells transfected with cDNA encoding tac(e)-gpI(mc) is the same as that in which C_6-NBD-Cer (F, arrows) is concentrated. (G and H) The small cytoplasmic vesicles in which tac immunoreactivity accumulates in cells transfected with cDNA encoding tac(e)-gpI(mΔc) are accessible to α2-macroglobulin. Representative colabeled vesicles are indicated by the small arrows. Bars, 20 μm.

chimeric protein lacked almost the whole of the cytosolic domain of gpI, tac-immunoreactive protein was not targeted to the TGN, but instead accumulated in small cytoplasmic vesicles. Since these vesicles were accessible to a marker, α2-macroglobulin, that enters cells by endocytosis, the tac-immunoreactive vesicles were identified as endosomes. These observations suggest that a domain found within the cytosolic tail of gpI is responsible for retaining the protein in the TGN. In the absence of the cytosolic tail, the protein traverses the Golgi apparatus and reaches endosomes.

In infected cells, the final site of viral envelopment has been demonstrated to be the TGN (9). Electron microscopic immunocytochemical observations revealed that gpI-immunoreactive protein becomes highly concentrated in the membrane of the concave face of a curvilinear TGN-derived vesicle. An abundance of viral tegument accumulates on the cytosolic side of this membrane. Viral nucleocapsids appear to insert into the cavity formed by the curving TGN membranes, which then wrap around the capsids and fuse, trapping the tegument material between the capsids and the gpI-containing membrane. The original concave face of the TGN-derived vesicle, in which gpI accumulates, thus becomes the viral envelope, while the original convex face contains MPR^{ci} immunoreactivity and becomes a transport vesicle. It is possible that the presence of Man 6-P on viral gps (7) is responsible for concentrating MPRs in the membrane that becomes the transport vesicle. This remains to be shown, but the transport of newly enveloped VZV in vesicles that contain MPRs has been proposed to be responsible for the routing of the virions to prelysosomes (late endosomes) and thus for the high rate of intracellular degradation of VZV that occurs prior to its secretion by infected cells in vitro and for the cell-associated nature of the virus (7–9, 26). The present study suggests that the concentration of gpI in the TGN that occurs in infected cells depends on a sequence (or sequences) that is present in the cytosolic domain of this molecule. Conceivably, tegument proteins, which lack signal sequences and thus are synthesized in the cytosol, may also bind to the cytosolic domain of gpI or other viral gps. Such binding would account for the observed accumulation of tegument protein adherent to the cytosolic face of the TGN membrane that is rich in gpI (9). The gp-tegument complex in this location could also account for the targeting of cytosolic nucleocapsids to the concave face of the TGN-derived envelopment vesicles. This formulation is strictly a model at this time. Although the hypothesis accounts for all observed data, neither the proposed binding of tegument proteins to the cytosolic domains of viral gps nor the proposed attraction of cytosolic nucleocapsids to gp-tegument complexes has been demonstrated. These critical elements of the model must be tested in future studies; however, the targeting of viral gps to the TGN as a result of a signal sequence or patch in the cytosolic domains of these molecules could be a critical element in determining the site and mechanism of envelopment of VZV.

Although it now seems likely that the cytosolic domain of gpI, the most abundant gp of the VZV envelope, contains the information necessary for concentrating that protein in the TGN, it cannot be assumed that an identical signal or even the same mechanism is responsible for targeting other gps. In fact, hydropathy plots of the sequences of other gps (6) suggest that only gpI, gpII, and gpIV have cytosolic tails of significant length; moreover, there is relatively little sequence identity in the putative cytosolic regions of these molecules. It is thus not yet clear what is responsible for routing gps other than gpI to the TGN. Signal sequences in different regions of the other gps may be responsible. Alternatively, other gps may not be independently targeted to the TGN, but instead they could be attracted to the site of viral envelopment by binding to gpI.

It should be noted that despite its accumulation in the TGN of transfected cells, gpI(wt) and the chimeric tac(e)-gpI(mc), which contains the TGN-targeting cytosolic domain, were not limited to this structure. Studies with cells that were not permeabilized clearly demonstrated that gpI(wt) and tac(e)-gpI(mc) were also present in the plasma membrane. This observation, also consistent with the behavior of gpI in infected cells, where a fraction is incorporated into the plasma membrane, implies that gpI(wt) and tac(e)-gpI(mc) are not anchored in the TGN. Instead, there must be membrane traffic in gpI(wt)-containing vesicles between the TGN and the plasma membrane. Since the progression of vesicles to the plasma membrane does not deplete the TGN of gpI(wt) or tac(e)-gpI(mc), however, it seems likely that the traffic is two way and that gpI(wt) and tac(e)-gpI(mc) probably return to the TGN from the plasma membrane to maintain the concentration of gpI(wt) or tac(e)-gpI(mc) in the TGN. This behavior of gpI(wt) is in marked contrast to that of tac(e)-gpI(mΔc), which lacks the TGN-targeting cytosolic domain and progresses to endosomes and/or lysosomes in a manner that results in its depletion from the TGN. The accumulation of this molecule in endosomes, where it codistributes with α2-macroglobulin suggests that tac(e)-gpI(mΔc) reaches the plasma membrane, like gpI(wt) and tac(e)-gpI(mc), and is retrieved by endocytosis, but then the absence of the TGN-targeting cytosolic domain causes tac(e)-gpI(mΔc) to be unable to return to the TGN and to remain in endosomes. The cytosolic protein(s) that recognize the TGN-targeting cytosolic domain of gpI and mediate its trafficking remain to be identified.

ACKNOWLEDGMENTS

This work was supported by Public Health Service grant AI 127187 from the National Institute of Allergy and Infectious Disease.

The authors thank Sharon Steinberg and Wanda Setlik for assistance.

REFERENCES

1. **Brown, W. J.** 1990. Cation-independent mannose 6-phosphate receptors are concentrated in trans Golgi elements in normal human and I-cell disease fibroblasts. Eur. J. Cell Biol. **51:**201–210.
2. **Brunetti, C. R., R. L. Burke, B. Hoflack, T. Ludwig, K. S. Dingwell, and D. C. Johnson.** 1995. Role of mannose-6-phosphate receptors in herpes simplex virus entry into cells and cell-to-cell transmission. J. Virol. **69:**3517–3528.
3. **Compton, T., and R. J. Courtney.** 1984. Virus-specific glycoproteins associated with the nuclear fraction of herpes simplex virus type 1-infected cells. J. Virol. **49:**594–597.
4. **Conibear, E., and B. M. F. Pearse.** 1994. A chimera of the cytoplasmic tail of the mannose 6-phosphate/IGF-II receptor and lysozyme localizes to the TGN where the bulk of the endogenous receptor is found. J. Cell Sci. **107:**923–932.
5. **Darlington, R. W., and L. H. Moss.** 1968. Herpesvirus envelopment. J. Virol. **2:**48–55.
6. **Davison, A. J., and J. E. Scott.** 1986. The complete DNA sequence of varicella-zoster virus. J. Gen. Virol. **67:**1759–1816.
7. **Gabel, C., L. Dubey, S. Steinberg, M. Gershon, and A. Gershon.** 1989. Varicella-zoster virus glycoproteins are phosphorylated during posttranslational maturation. J. Virol. **63:**4264–4276.
8. **Gershon, A., L. Cosio, and P. A. Brunell.** 1973. Observations on the growth of varicella-zoster virus in human diploid cells. J. Gen. Virol. **18:**21–31.
9. **Gershon, A. A., D. L. Sherman, Z. Zhu, C. A. Gabel, R. T. Ambron, and M. D. Gershon.** 1994. Intracellular transport of newly synthesized varicella-zoster virus: final envelopment in the *trans*-Golgi network. J. Virol. **68:**6372–6390.
10. **Griffiths, G., P. Hoflack, K. Simons, I. Mellman, and S. Kornfeld.** 1988. The mannose 6-phosphate receptor and the biogenesis of lysosomes. Cell **52:**329–341.
11. **Griffiths, G., and P. Rottier.** 1992. Cell biology of viruses that assemble along the biosynthetic pathway. Semin. Cell Biol. **3:**367–381.
12. **Ho, S. N., H. D. Hunt, R. M. Horton, J. K. Pullen, and L. R. Pease.** 1989. Site-directed mutagenesis by overlap extension using the polymerase chain

reaction. Gene **77:**51–59.
13. **Hobman, T. C., M. L. Lundstrom, and S. Gillam.** 1990. Processing and intracellular transport of rubella virus structure proteins in Cos cells. Virology **178:**122–133.
14. **Hobman, T. C., L. Woodward, and M. G. Farquhar.** 1993. The rubella virus E2 and E1 spike glycoproteins are targeted to the Golgi complex. J. Cell Biol. **121:**269–281.
15. **Kornfeld, R., and S. Kornfeld.** 1985. Assembly of asparagine-linked oligosaccharides. Annu. Rev. Biochem. **54:**631–646.
16. **Kornfeld, S.** 1987. Trafficking of lysosomal enzymes. FASEB J. **1:**462–468.
17. **LaRussa, P., O. Lungu, I. Hardy, A. Gershon, S. P. Steinberg, and S. Silverstein.** 1992. Restriction site polymorphism of polymerase chain reaction products from vaccine and wild-type varicella-zoster virus isolates. J. Virol. **66:**1016–1020.
18. **Marquardt, T., and A. Helenius.** 1992. Misfolding and aggregation of newly synthesized proteins in the endoplasmic reticulum. J. Cell Biol. **117:**505–513.
19. **Montalvo, E., R. Parmley, and C. Grose.** 1985. Structural analysis of the varicella-zoster virus gp98-gp62 complex: posttranslational addition of N-linked and O-linked oligosaccharide moities. J. Virol. **53:**761–770.
20. **Morgan, C., S. A. Ellison, H. M. Rose, and D. H. More.** 1954. Structure and development of viruses as observed in electron microscope. I. Herpes simplex virus. J. Exp. Med. **100:**195–202.
21. **Morgan, C., H. M. Rose, M. Holden, and E. P. Jones.** 1959. Electron microscopic observations on the development of herpes simplex virus. J. Exp. Med. **110:**643–656.
22. **Pagano, R. E., M. A. Sepanski, and O. C. Martin.** 1989. Molecular trapping of a fluorescent ceramide analogue at the Golgi apparatus of fixed cells: interaction with endogenous lipids provides a trans-Golgi marker for both light and electron microscopy. J. Cell Biol. **109:**2067–2079.
23. **Petterson, R. F.** 1991. Protein localization and virus assembly at intracellular membranes. Curr. Top. Microbiol. Immunol. **170:**67–106.
24. **Sharon, J., C. Y. Kao, and S. R. Sompuram.** 1993. Oligonucleotide-directed mutagenesis of antibody combining sites. Int. Rev. Immunol. **10:**113–127.
25. **Stephens, E. B., and R. W. Compans.** 1988. Assembly of animal viruses at cellular membranes. Annu. Rev. Microbiol. **42:**489–516.
26. **Weller, T. H., and H. M. Witton.** 1958. The etiologic agents of varicella and herpes zoster. Serological studies with the viruses as propagated in vitro. J. Exp. Med. **108:**869–890.
27. **Whealy, M. E., J. P. Card, R. P. Meade, A. K. Robbins, and L. W. Enquist.** 1991. Effect of brefeldin A on alphaherpesvirus membrane protein glycosylation and virus egress. J. Virol. **65:**1066–1080.

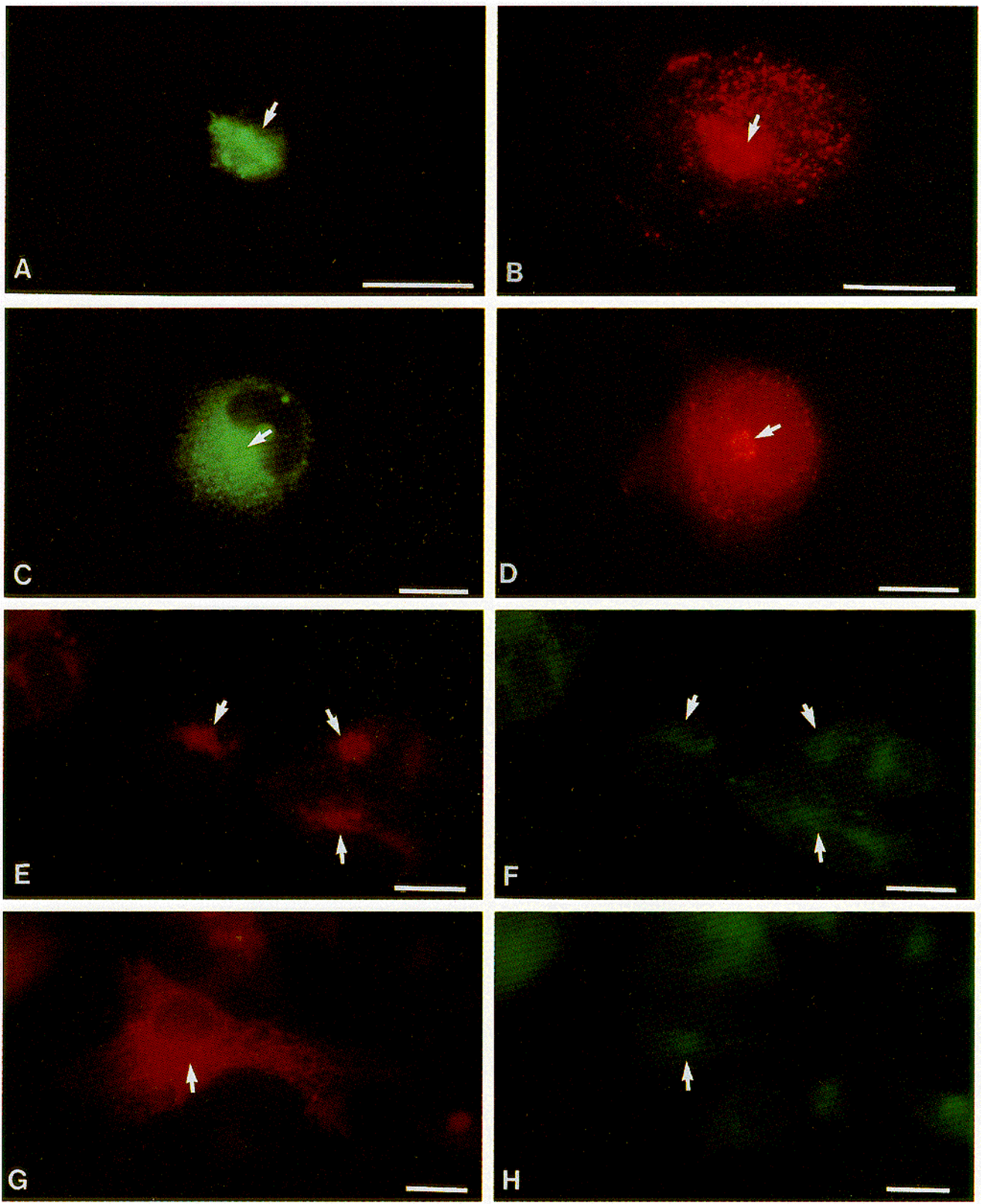
A
B
C
D
E
F
G
H

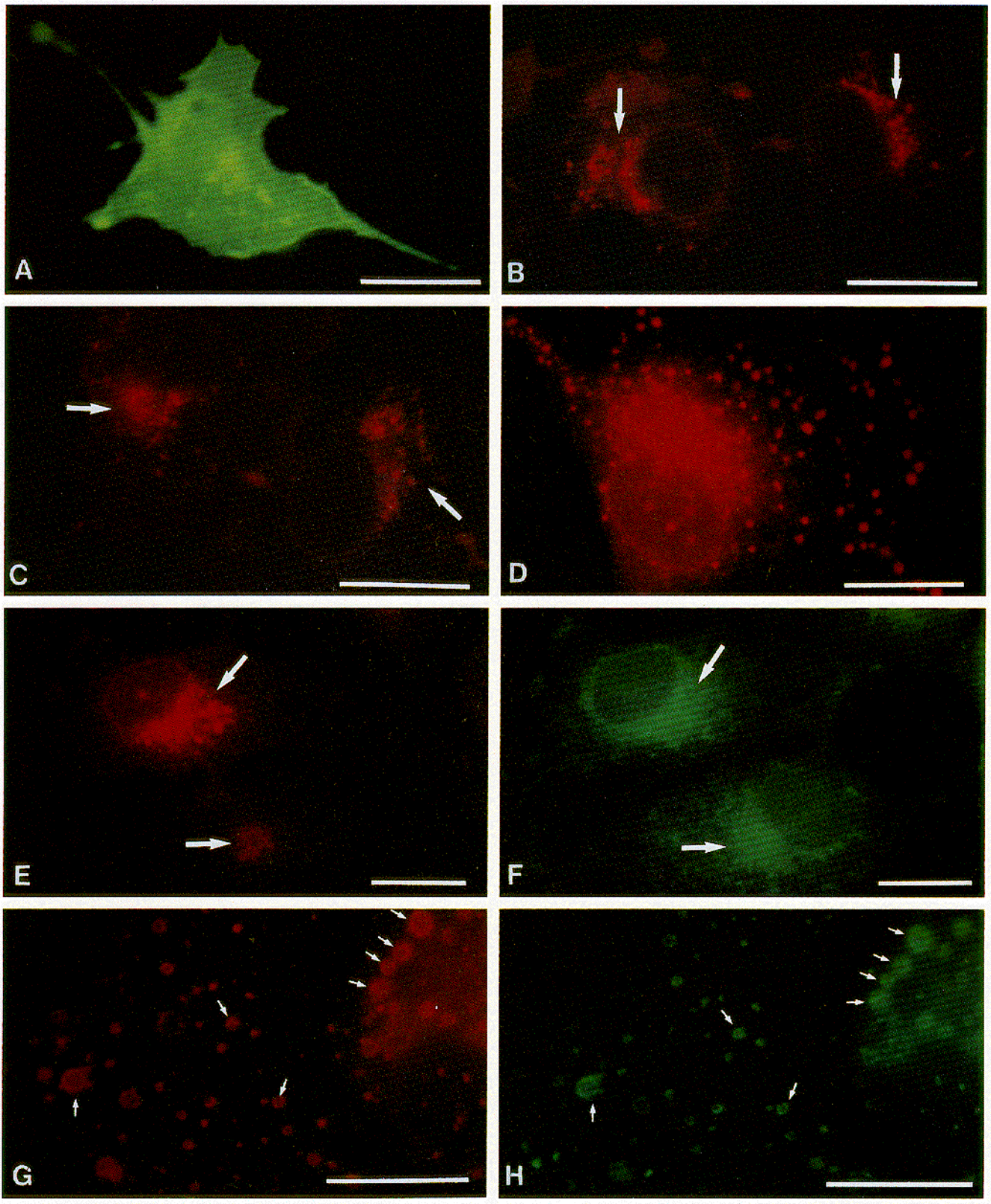
A
B
C
D
E
F
G
H